ACS APPLIED MATERIALS & INTERFACES

Research Article

www.acsami.org

Impact of Copper Overpressure on the Synthesis of Hexagonal Boron Nitride Atomic Layers

Michael S. Bresnehan,[†,‡,§] Ganesh R. Bhimanapati,[†,§] Ke Wang,[∥] David W. Snyder,[‡,⊥] and Joshua A. Robinson*[,†,§,∥]

[†]Department of Materials Science and Engineering, [‡]Electro-Optics Center, [§]Center for 2-Dimensional and Layered Materials, [∥]Materials Research Institute, and [⊥]Department of Chemical Engineering, The Pennsylvania State University, University Park, Pennsylvania 16802, United States

S *Supporting Information*

ABSTRACT: Hexagonal boron nitride (h-BN) atomic layers are synthesized on polycrystalline copper foils via a novel chemical vapor deposition (CVD) process that maintains a vapor-phase copper overpressure during growth. Compared to h-BN films grown without a copper overpressure, this process results in a >10× reduction of 3-dimensional BN fullerene-like surface features, a reduction of carbon and oxygen contamination of 65% and 62%, respectively, an increase in h-BN grain size of >2×, and an 89% increase in electrical breakdown strength.

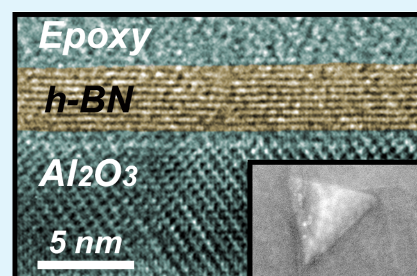

KEYWORDS: *hexagonal boron nitride, h-BN, graphene, CVD, dielectrics*

INTRODUCTION

Hexagonal boron nitride (h-BN) is an excellent candidate for dielectric integration with graphene electronics.[1−8] High surface optical phonon modes allow for minimal scattering of graphene's charge carriers from surface optical phonons,[1,6,7] while strong in-plane covalent bonding reduces the density of charged impurities that may be introduced at the graphene/h-BN interface, reducing Coulombic scattering in graphene.[1,9] Chemical vapor deposition (CVD) of h-BN on transition metals is the most common synthesis technique for large scale h-BN dielectrics. Copper, having a 2.3% (111) lattice mismatch with h-BN[10] is one of the most common transition metal substrates for CVD synthesis of h-BN and, like Ni, forms strictly 1 × 1 commensurate h-BN layers.[10] Growth of h-BN on Cu generally results in a polycrystalline film with domain sizes <10 nm.[11−13] Therefore, the crystallinity is not as high as h-BN films grown on Ni, where domains >1 μm have been obtained.[14] However, Yang et al.[15] found that h-BN films grown on Ni foils are generally more leaky as a dielectric layer due to incomplete regions present at Ni grain boundaries.[15] Therefore, growth of h-BN on Cu foils represents a suitable approach for large scale device development. Additionally, growth of h-BN on Cu is not a self-limited growth process (unlike graphene growth on Cu), where the film thickness of h-BN grown on Cu can be controlled through tailoring of the growth parameters.[11,13,16] The control of layer thickness is critical for gate dielectric applications, where the tunneling currents were found to be excessive for single crystal exfoliated h-BN flakes less than four layers thick.[17,18] Despite the well documented research on h-BN growth on Cu substrates,[10−13,15,16] the growth mechanisms of CVD grown h-BN are not fully understood and several growth-related issues exist which can impact graphene device performance, such as (1) impurity scattering from dangling bonds of 3D nanoparticles, (2) surface roughness scattering from wrinkles induced during growth, and (3) current leakage through nanocrystalline domain boundaries. Here, we examine the growth mechanisms of h-BN on Cu foils and present a route toward the resolution of these issues.

Recently, Li et al.[19] demonstrated synthesis of graphene on copper substrates via CVD in a copper enclosure, which resulted in monolayer graphene with domain size increases of ∼30× and a lower density of adlayers compared to non-enclosed graphene growth.[19] This is due to a lower partial pressure of methane (leading to a reduced density of nucleation sites) as well as an improved growth environment through creation of a static Cu overpressure inside the copper enclosure. We have investigated a similar concept for the growth of h-BN on Cu. A simple Cu enclosure was utilized to provide the Cu overpressure. This enclosure was made by wrapping a sheet of copper (99.8% purity) around a quartz boat holding up to six 10 × 10 mm^2 Cu foils (Supporting Information, Figure S1). We show that this process enhances structural, chemical, and dielectric properties of h-BN films. The present results ultimately show an ∼11× reduction of 3-dimensional fullerene-like h-BN surface features, a reduction of carbon and oxygen contamination of 65% and 62%, respectively, an increase in h-BN grain size of >2×, and an 89% increase in

Received: June 16, 2014
Accepted: September 8, 2014
Published: September 8, 2014

ACS Publications © 2014 American Chemical Society

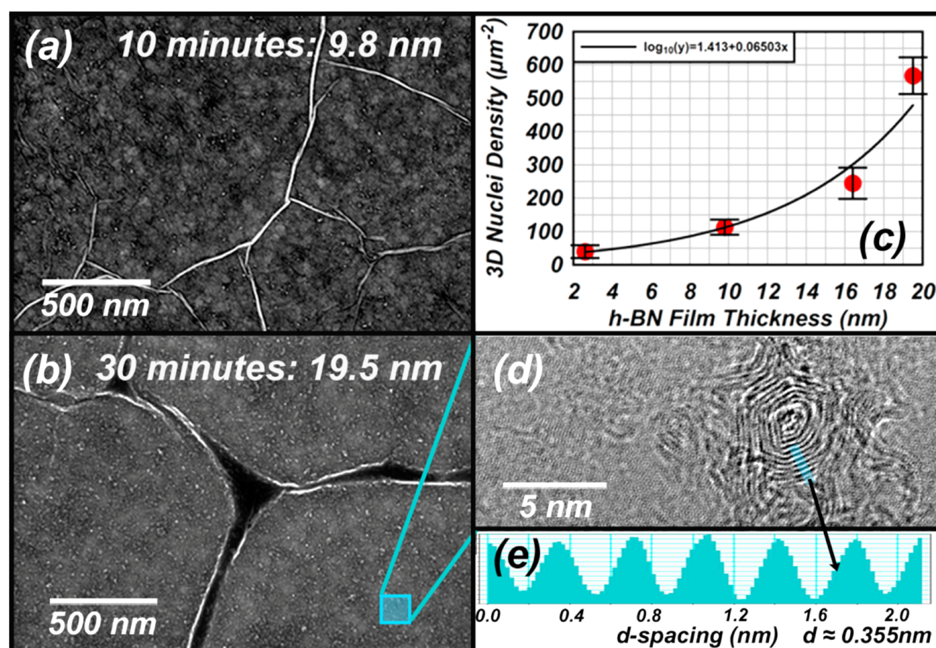

Figure 1. FESEM images of (a) ∼10 nm and (b) ∼20 nm h-BN films as-grown on Cu substrates *without* a Cu enclosure show the presence of stress induced wrinkling and 3D formations. (c) Density of 3D formations versus h-BN film thickness indicates that the nucleation rate of these 3D features increases with increasing thickness, possibly due to increased density of defects and domain boundaries at higher film thickness. (d) Plan-view TEM image of a 3D formation shows that the h-BN planes propagate normal to the Cu surface and form in a BN fullerene-like structure. (e) *d*-spacing of the layers in the 3D formation show a *d*-spacing matching that of h-BN.

electrical breakdown strength coupled with a decrease in leakage current density of nearly 4 orders of magnitude. Additionally, we provide evidence that the growth of h-BN on Cu proceeds similarly to the Stranski−Krastanov growth mode.[20]

RESULTS AND DISCUSSION

Figure 1a and b show scanning electron microscopy (SEM) images of a 10 nm h-BN film (Figure 1a) and a 20 nm h-BN film (Figure 1b) as-grown on Cu *without* the use of a copper enclosure. Clearly recognizable is the presence of wrinkles across the film surface, similar to those observed elsewhere.[6,16] Wrinkling results from compressive stresses induced from the anisotropic thermal expansion of h-BN, where a negative coefficient of thermal expansion (CTE) exists in the plane of bonding.[21] In addition, three-dimensional (3D) island formations appear evenly distributed across the film surface (Figure 1a and b). The 3D features nucleate randomly, and increase in density by >14× (from ∼40 (±19) nuclei/μm^2 to ∼568 (±55) nuclei/μm^2) as film thickness increases from ∼3 to ∼20 nm, as shown in Figure 1c.

The growth of 3D nuclei is hypothesized to proceed by one of two possible mechanisms. The first is the nucleation and precipitation of nanoparticles in the gas-phase onto the growing h-BN film and the second is the nucleation of nanoparticles on the h-BN film surface at surface defects and grain boundaries. In the case of gas-phase nucleation, the density of these 3D particulates would be expected to increase linearly with time. As shown in Figure 1c, however, the increase in 3D nuclei density increases exponentially, indicating a higher nucleation rate of these features at higher film thicknesses. This suggests that the 3D features are nucleating at defects on the film surface, likely due to degradation of crystallinity with increasing thickness as verified with cross-sectional transmission electron microscopy (TEM) in the Supporting Information (Figure S2). To examine these 3D formations further, plan-view TEM was utilized (Figure 1d) and indicates that the 3D nuclei are h-BN layers growing perpendicular to the Cu substrate surface, in contrast to the underlying film, which propagates parallel to the growth surface (Supporting Information Figure S2). Furthermore, these h-BN layers appear to form an onion-like structure. The *d*-spacing (Figure 1e) was measured to be 0.355 nm, similar to bulk h-BN (0.333 nm),[22] confirming the 3D nuclei are h-BN. These features are notably similar to BN fullerenes, where literature has shown that BN fullerenes form more preferentially from turbostratic BN, which displays small domain sizes and a high density of defects and dangling bonds compared to well-ordered h-BN.[23−25]

X-ray photoelectron spectroscopy (XPS), detailed in the Supporting Information, indicates that oxygen contamination is present in films grown *without* a copper enclosure (Supporting Information Figure S3). Upon deconvolution of the XPS data, two peaks are found to make up the B 1s spectra. The peak at ∼190.45 eV (red peak, Supporting Information Figure S3a) is the main bonding configuration of the film and correlates to a boron atom bonded to three nitrogen atoms in the typical h-BN lattice structure. The second peak at ∼191.52 eV (blue peak, Supporting Information Figure S3a) correlates to a boron atom bonded to nitrogen and oxygen atoms. Since oxygen has a higher electronegativity than nitrogen, this bonding configuration will result in the formation of a peak shifted to higher binding energies. Therefore, this peak implies that there is partial bonding of oxygen to boron and can be assigned to a BN_xO_y configuration that accounts for 5.46% of the total bonding in the h-BN lattice. The presence of oxygen impurities in the as-grown BN film further corroborates the theory that the observed 3D nuclei present on the h-BN film surface are BN fullerene structures. BN fullerenes are composed of

hexagons and pentagons that would ultimately form thermodynamically unfavorable B−B and N−N bonds. Therefore, BN fullerenes require the incorporation of substitutional oxygen into the BN lattice to form stable B−O bonds at the pentagon and hexagon boundaries.[23] Further research is required to fully understand the exact growth mechanisms of these 3D formations; nevertheless it is evident that these features will negatively impact graphene device performance. An obvious adverse effect would be increased surface roughness scattering when these films are used as a supporting substrate to graphene or transition metal dichalcogenides (TMDC's). Additionally, having the basal plane normal to the h-BN film, these 3D nuclei have dangling bonds at the terminations of the in-plane σ-bonds. It is expected that impurities will readily absorb at these sites and may lead to reduced resistivity of the h-BN film when used as a gate dielectric and lead to increased impurity scattering when used as a supporting dielectric substrate. Therefore, a reduction or elimination of these surface defects would presumably be highly beneficial to the dielectric performance of CVD grown h-BN films.

To investigate the effects on the structural and chemical properties of the h-BN, films are grown with and without the use of a copper enclosure for various growth times, but were otherwise grown under the same conditions. The h-BN film thickness as a function of growth time is shown in the Supporting Information (Figure S4) for films grown with and without the use of a copper enclosure. The use of a copper enclosure during h-BN growth resulted in a 53.7% decrease in growth rate. This reduction in growth rate is due to the gas-phase environment surrounding the Cu substrates during growth. Dalton's law states that the total pressure of a mixture of gases is equal to the sum of the partial pressures of the individual gases in the mixture, such that[26] $P_{tot} = P_1 + P_2 + P_3 + ...$ For the growth configuration utilizing the copper enclosure, it can be assumed to be an open system where the total pressure inside the copper enclosure is equal to the total pressure outside of the enclosure. Given that the vapor pressure of Cu is relatively high for a transition metal (7.5×10^{-5} Torr at 1000 °C),[27] the nearly static partial pressure of copper inside the enclosure would be significantly higher than that above Cu samples without a copper enclosure. Therefore, to satisfy Dalton's equation, the partial pressures of the remaining gas-phase species, including BN precursors, such as borazine and diborane, would be reduced within the copper enclosure. A reduced partial pressure of BN precursors leads to a reduction in the impingement flux of gas-phase precursors. This is illustrated by $\Phi = 3.513 \times 10^{22}(P_i/(MT)^{1/2})$, where Φ is the impingement flux (molecules/cm^2-s), P_i is the partial pressure of gas species (Torr), M is the molecular weight of gas species, and T is the temperature (°C).

The reduced flux of h-BN precursors would lead to a reduction in adatom surface density, n_a (cm^{-2}), by $n_a = \tau_S \Phi$, where τ_s (s^{-1}) is the adatom lifetime.[20] Additionally, the adatom surface density is directly proportional to the nucleation rate, $\dot{N}$ (nuclei/cm^2-s).[20] The grain diameter, l_g (cm), is then given by $l_g \propto (\dot{G}/\dot{N})^{1/3}$, where $\dot{G}$ (cm/s) is the linear growth rate of the grain.[20] This suggests then that a decrease in partial pressure of BN precursors through the use of a copper enclosure should enhance the domain size of the h-BN film, which is highly desirable since small domain sizes are often reported for growth of h-BN on Cu foils and lead to increased leakage currents.[11−13] Figure 2 shows SEM images detailing the evolution of grain size with growth time, as a function of film thickness (measured via optical ellipsometry) for h-BN films grown using a copper enclosure.

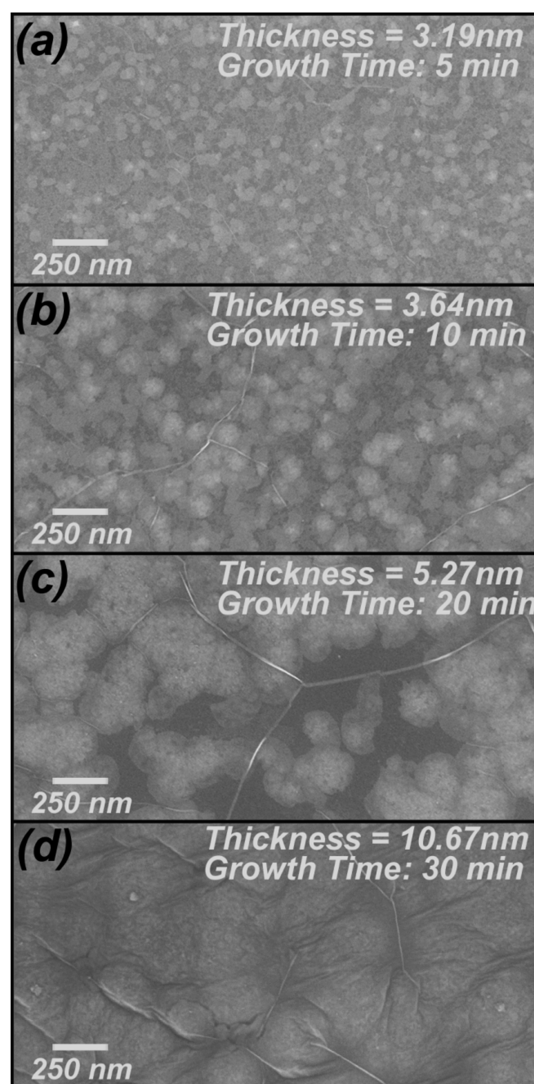

Figure 2. Top−down FESEM images of h-BN films grown via CVD on copper foils, *with* a Cu enclosure, at various growth times and subsequently transferred to Si(111) substrates. The h-BN film thickness increases progressively from panel a to d.

Island formation is readily discernible with SEM (Figure 2), and AFM (Supporting Information, Figure S5), where islands increase in size and decrease in density as the film thickness increases. At a film thickness of ∼10 nm, grains appear to be nearly coalesced and individual islands become more difficult to distinguish. The Cu enclosure results in a >2.3× increase in h-BN island size at similar film thicknesses (∼5 nm), where the islands are an average of 177.2 nm (±3.6 nm) for the enclosed growth (Figure 2c) and 75.8 nm (±6.0 nm) for the non-enclosed growth (not shown). This is due to the increased flux of BN precursors on the Cu surface for the *non-enclosed* growth, where the diffusion mean free path (L) is decreased by $\approx (D/\Phi)^{1/6}$, where D is the diffusion coefficient. Therefore, the probability of adatoms forming new nucleation sites, rather than attaching to existing nuclei, is increased compared to the *enclosed* growth, which results in a high density of small h-BN islands (as shown in Figure 1a and b). Additionally, XPS analysis is detailed extensively in the Supporting Information (Figure S6) and confirms an enhancement of the chemical

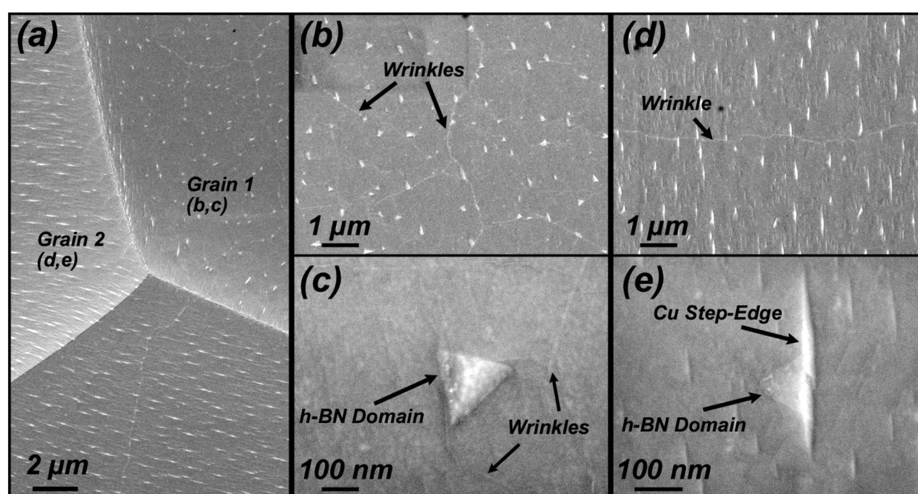

Figure 3. FESEM images of an h-BN film grown with a copper enclosure for a growth time of 2.5 min. (a) Low magnification FESEM image showing multiple Cu grain orientations. (b, c) High magnification images of Grain 1 showing the formation of triangular domains oriented randomly over an h-BN monolayer. (d, e) High magnification images of Grain 2 showing the formation of triangular domains nucleating preferentially from Cu step-edges over an h-BN monolayer.

properties of h-BN films grown *with* a copper enclosure, where carbon and oxygen content decreased by 62% and 65%, respectively, compared to films grown *without* a copper enclosure. This is also a result of Dalton's Law, where the partial pressures of impurity gases (such as water vapor and backstreamed pump oil) will be decreased with the increased copper overpressure. As a result, films grown *with* a Cu enclosure remain nearly free of 3D nuclei, which require oxygen to form thermodynamically.[23] At a film thickness of ~20 nm, the density of 3D nuclei on Cu-enclosed films is decreased by ~11× (from ~568(±55) nuclei/μm^2 to ~52(±15) nuclei/μm^2) compared to a non-enclosed film of similar thickness.

Unlike previous reports,[12,16] the shape of the h-BN grains observed in Figure 2 appear circular. Kim et al.[16] suggest that triangles are more energetically favorable for h-BN growth since nitrogen-terminated edges have lower edge energy than boron-terminated edges. However, for the multilayer h-BN films shown in Figure 2, h-BN triangular domains are not observed, suggesting that the circular islands are likely composed of many nanocrystalline domains. To understand the growth mechanisms of the films presented in this work, the growth time was reduced further to grow a monolayer h-BN film. Figure 3 shows SEM images taken of an h-BN film as-grown on Cu after 2.5 min of growth with the use of a Cu enclosure. Figure 3a is a low magnification image showing three different Cu grains. Figure 3b shows a high magnification image of Grain 1 (top right corner of Figure 3a) and shows several randomly oriented triangular h-BN domains nucleating over a complete monolayer, as apparent from the wrinkling of the underlying monolayer. Figure 3c shows a higher magnification image of a triangular h-BN domain from Grain 1 with a length (tip of triangle to center of base) of approximately 195 nm. The triangular domains observed on Grain 1 appear to nucleate preferentially from surface wrinkles (likely at defects or dangling bonds at wrinkle edges) suggesting that the wrinkling of this particular grain may occur *during* growth, despite the belief that surface wrinkling occurs during postgrowth cooling of the sample.[21] This may be due to the orientation of this particular grain. It has been previously reported that the (111) face of Cu is an ideal substrate for h-BN growth because of their lattice mismatch of only 2.3%, where Cu(111) has a lattice constant of 2.56 Å[28] and h-BN has a lattice constant of 2.50 Å.[22] However, Cu(100) has a lattice constant of 3.61 Å,[22] giving a lattice mismatch with h-BN of 30.8%. Therefore, for a polycrystalline Cu foil, the local lattice mismatch will vary depending on grain orientation. It is likely that the orientation of Grain 1 is not (111), leading to a larger lattice mismatch that results in wrinkling during growth. Since the wrinkles propagate in random directions, h-BN domains nucleating from these wrinkles will be randomly oriented, as observed in Figure 3b.

In contrast, Figure 3d and e show high magnification images from Grain 2 (top left corner of Figure 3a). Unlike Grain 1, where the h-BN triangular domains were randomly oriented, h-BN grown on Grain 2 shows preferential nucleation of h-BN triangles from crystallographic Cu step-edges. The wrinkling observed in Figure 3d indicates that again, these domains are forming over a complete monolayer. Interestingly, however, the density of wrinkles in Grain 2 is significantly less than in Grain 1, where the overall length of observable wrinkles was measured to be 26.6 μm in Grain 1 (Figure 3b) and 10.4 μm in Grain 2 (Figure 3d), indicating a 61% higher wrinkle density in Grain 1. It is likely that Grain 2 is a Cu(111) grain, where a small lattice mismatch exists. Closer inspection of the SEM images reveals that the triangular domains do not nucleate at the large wrinkle observed in Grain 2, indicating that film wrinkling of Grain 2 occurred only during cooling to compensate for the mismatch in CTE between h-BN and Cu. In this case, nucleation of secondary triangular domains over the original monolayer occurs at crystallographic step-edges rather than at wrinkle edges, as shown in Figure 3e. The step-edges likely provide energetically favorable nucleation sites due to an increased density of dangling bonds, even for growth of the second h-BN layer. This suggests that improved orientation texturing of h-BN monolayers and bilayers can be controlled through selection of the Cu orientation. It is difficult to determine the orientation of Grains 1 and 2 based on morphological observation alone. A technique such as orientation imaging microscopy (OIM) would be required for precise indexing. However, RMS surface roughness limits (typically <1 nm) prevent its use for the Cu foils used in this work.

On the basis of the observed morphological features, a potential nucleation and growth model can be proposed. Figure

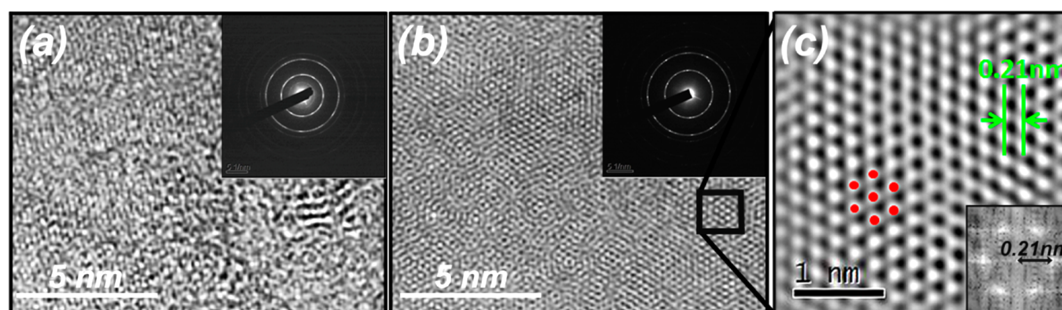

Figure 4. (a, b) Plan view TEM of an h-BN film grown *without* and *with* the use of a Cu enclosure, respectively. The corresponding diffraction patterns of (a) and (b) are shown as insets, and indicate that the use of a Cu enclosure during growth resulted in higher degree of crystallographic texturing and larger domains. (c) High magnification TEM image of (b) showing the commensurate hexagonal structure. Inset shows the calculated FFT pattern from the TEM image of (c) and was used to measure *d*-spacing.

3 verifies that the h-BN films grown in this work do initially nucleate as triangular single-crystal domains. It is widely believed that the first monolayer forms rapidly because of the high surface reactivity and diffusion rate of borazine on Cu (as well as the high initial precursor concentrations observed via mass spectrometry in the Supporting Information (Figure S7)).[29] However, the surface reactivity of BN precursors such as borazine on h-BN (compared to Cu) is poor.[29] This would lead to a dramatic reduction in surface diffusion of BN precursors, and thus a reduction of h-BN domain size, over the initial h-BN monolayer. This corroborates with the work of Kim et al.,[16] who show that the size of the triangular domains decrease significantly after the formation of a complete monolayer. It is apparent from the work of Kim et al.[16] and the results shown in this work (Figure 3) that single crystal triangular domains can form even after the initial monolayer. Additionally, Figure 3d shows that even after the formation of the original monolayer, subsequent h-BN triangles nucleate from Cu surface features such as step-edges. This suggests that these triangular domains retain some binding energy to the Cu substrate for at least the first two (possibly more) layers. This binding energy would decrease exponentially with increasing layer thickness, however, and may explain the transition from the large (~200 nm) single-crystal triangular domain growth observed in Figure 3 to the small (~20 nm) circular island growth observed for thicker films in Figure 2. After the first few h-BN layers, the binding energy between impinging BN precursors and the Cu substrate is negligible and subsequent h-BN growth nucleates as nanocrystalline domains (possibly at domain edges or defects) rather than large single-crystal h-BN triangles, due to the decreased adatom diffusion. These nanocrystalline domains eventually nucleate off of each other and form small circular islands. This suggests that h-BN growth on Cu proceeds similarly to the Stranski−Krastanov growth mode, where island growth becomes favorable to layer-by-layer growth after the first few layers due to a decrease in film−substrate binding energy with increasing thickness.[20] This transition from well-ordered h-BN layers to nanocrystalline/turbostratic BN layers was also observed by Ismach et al. for h-BN growth on Ni and Sapphire,[30] suggesting that the proposed Stranski−Krastanov growth mode may be valid for CVD growth of h-BN on various substrates.

The observed morphological benefits with use of a copper enclosure during h-BN growth ultimately lead to an improvement in crystallographic texturing, as observed with plan-view TEM on ~20 nm thick h-BN films grown *without* (Figure 4a) and *with* (Figure 4b) the use of copper enclosure. The observed domain size is small (~5 nm) for both growth configurations. This is expected since, based on the proposed growth model and cross-sectional TEM observations (Supporting Information, Figure S2), the surfaces of these ~20 nm thick films are likely composed of nanocrystalline/turbostratic BN structures, where a transition to turbostratic BN growth was found to occur after ~15 layers (see Supporting Information Figure S2). However, the crystallographic texturing of the enclosed sample is enhanced compared to the non-enclosed sample, as apparent from the selected area diffraction patterns (SAD), shown in the insets of Figure 4a and b. Here, broad rings and weak diffraction spots are observed for the non-enclosed sample while the SAD pattern of the enclosed sample appears much sharper, indicating that the crystallinity of this film is improved. Additionally, the non-enclosed film shows areas where the *c*-axis propagates perpendicular to the growth surface, similar to the TEM analysis of the 3D nuclei shown previously in Figure 1d. In contrast, h-BN grown *with* a copper enclosure shows an absence of non-basal layers. In both cases the *d*-spacing is ~0.21 nm, matching the interatomic distance in the (0001) plane of bulk h-BN.[22]

To investigate the insulating behavior of the h-BN films as a function of thickness and growth configuration (with or without a Cu enclosure), electrical breakdown measurements were performed. It has been previously reported that bulk h-BN typically has a breakdown field in the range of $2-6 \times 10^6$ V/cm.[31] However, breakdown fields reported for exfoliated h-BN have been reported at $10-15 \times 10^6$V/cm, due to the pristine single crystal nature of exfoliated h-BN flakes.[17,18] In these reports, it was found that exfoliated h-BN flakes of less than 4 layers experienced significant tunneling currents. However, the breakdown characteristics of h-BN films grown by CVD on Cu have not been thoroughly explored. For these experiments, the breakdown field was considered to be the voltage field (V/cm) where the current density reached 10 A/cm^2.

Breakdown analysis was performed on h-BN films of similar thicknesses, but grown under different growth configurations. Alternatively, the breakdown of h-BN films as a function of thickness is shown in the Supporting Information, Figure S8. Figure 5 shows the log−log plots of current density versus voltage field for ~20 nm thick h-BN films grown with or without the use of a copper overpressure and shows a significant difference between the two growth configurations. For the ~20 nm h-BN film grown *with* the Cu enclosure, breakdown occurs at 1.34×10^6 V/cm. Conversely, for the ~20 nm thick h-BN film growth *without* the Cu enclosure, breakdown occurs at 7.09×10^5 V/cm. This indicates an

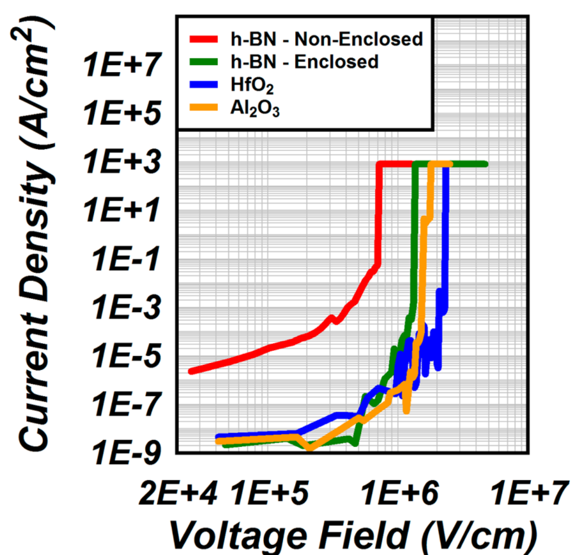

Figure 5. Current density vs voltage field showing the breakdown characteristics of 20 nm h-BN films grown with and without the use of a copper enclosure. The breakdown characteristics of two 30 nm thick high-*k* dielectrics, Al_2O_3 and HfO_2, are also shown. The h-BN film grown with the copper enclosure shows similar leakage currents and only a slightly lower breakdown field compared to high-*k* dielectrics, while the h-BN film grown without the copper enclosure shows significantly higher leakage currents and a reduced breakdown field.

increase in h-BN breakdown field of 89% when grown with the use of a Cu enclosure. Additionally, the current density at a voltage field of 1×10^5 V/cm increases by over 4 orders of magnitude (from 3.40×10^{-9} to 2.04×10^{-5} A/cm^2) when h-BN is grown *without* the use of a Cu enclosure. This indicates that the density of conduction paths is significantly increased in the h-BN film grown *without* the use of a Cu enclosure. This could be a result of an increased density of domain boundaries due to the decreased crystallinity observed in Figure 4, or an increase in conductivity because of the increased carbon content of the h-BN film grown *without* a Cu enclosure (see Supporting Information, Figure S6). For comparison, the breakdown characteristics of two high-k dielectrics typically used as dielectrics in graphene devices (Al_2O_3 and HfO_2) were plotted with the h-BN results. Both of these high-k dielectrics were ~30 nm thick and deposited via e-beam evaporation. It was found that the current densities were very similar up to ~1 $\times 10^6$ V/cm, indicating that the leakage currents for h-BN films grown *with* the use of a Cu enclosure are on par with these two high-k dielectrics. As expected, however, the breakdown fields for the high-k dielectrics were slightly higher than the h-BN film, where breakdown of the Al_2O_3 and HfO_2 films occurred at 1.76×10^6 and 2.32×10^6 V/cm, respectively, due to their superior dielectric strength. This indicates that h-BN dielectrics grown on Cu foils *with* the use of a Cu enclosure have breakdown strengths only moderately lower than these common high-k dielectrics, where its breakdown strength was found to be ~24% and ~42% less than Al_2O_3 and HfO_2, respectively.

■ CONCLUSIONS

The use of a copper enclosure during the pregrowth anneal and growth of h-BN films has been shown to be highly beneficial for h-BN synthesis on copper substrates. It was found that the Cu enclosure acted to reduce the partial pressure of gas-phase BN precursors through the creation of a static Cu vapor overpressure above the Cu foil samples. This not only resulted in a ~54% decrease in growth rate compared to h-BN growth without a Cu enclosure, but also in a >2.3× increase in h-BN island size at similar film thicknesses (~5 nm) because of a reduced flux of BN precursors to the Cu substrate, which ultimately led to an enhancement in film crystallinity. Additionally, this work proposed a growth model where h-BN proceeds via the nucleation of nanocrystalline islands over an original monolayer (Stranski−Krastanov growth mode),[20] where initial single crystal triangular domains were ~200 nm in diameter. Cross-sectional TEM analysis was used to verify the proposed growth model and showed well ordered and laminar h-BN layers at a thickness of 5 nm. However, at a thickness of >10 nm, a clear transition from layered growth to turbostratic growth was observed, indicating that the crystallinity of these films degrades significantly after full coalescence of h-BN islands. It was found that the copper enclosure led to an ~11× reduction in the density of 3D fullerene-like surface features (at a film thickness of 20 nm), likely due to the improved crystallinity and the reduction of oxygen contamination, where XPS shows that the concentrations of oxygen and carbon impurities were reduced by 65% and 62%, respectively. Because of these improvements, h-BN films grown *with* a Cu enclosure were found to result in an 89% increase in breakdown strength and a decrease in leakage current density of nearly 4 orders of magnitude at a voltage field of 1×10^5 V/cm for ~20 nm thick films, compared to non-enclosed films. It should be noted that these results also suggest that the Cu enclosure may not be needed if the partial pressure could be reduced by alternative techniques, such as incorporation of a pressure-based mass flow controller to accurately control the concentration of gas-phase precursors introduced into the system. Unfortunately, at the time of this work, such a growth configuration was not available. However, use of the Cu enclosure configuration clearly illustrates the benefits of a reduced precursor partial pressure for h-BN growth on copper substrates.

■ EXPERIMENTAL SECTION

Hexagonal boron nitride was grown on copper substrates, 25 μm thick 99.999% purity (metals basis) Cu foils (Alfa Aesar, part no. 10950), via a thermal CVD process in a 1 in. diameter horizontal tube furnace, similar to previously reported methods.[11] The Cu substrates were cleaned prior to h-BN growth using an acetone/isopropyl alchohol (IPA) solvent clean, followed by 20% acetic acid (JT Baker, part no. 9503-05) to remove the copper's native oxide. Ammonia borane (NH_3BH_3) (Sigma-Aldrich, part #682098) was used as the precursor for h-BN growth, upon sublimation at 135 °C. A pregrowth anneal is performed at 1000 °C and 350 mTorr for 2 h to remove any additional oxide that may have regrown following cleaning and to increase the grain size of the starting Cu surface via a thermal surface reconstruction.[32,33] For many growth runs, the Cu samples were encapsulated in a Cu enclosure by wrapping the boat and samples with 99.8% purity Cu foil (Alfa Aesar, part #13382), shown in the Supporting Information (Figure S1). After the pregrowth anneal, the sublimated ammonia borane was transported into the tube furnace by an H_2/N_2 carrier gas (Here the carrier flow was 5% of the total flow rate, where the total flow rate was 30 sccm). Growth occurs at 1000 °C and 350 mTorr with growth times ranging between 2.5 and 30 min, depending on desired film thickness. After growth is completed, the furnace is shut off, the ammonia borane source is closed, and the samples are allowed to slowly cool to room temperature under H_2/N_2 flow (15% H_2 mixture). Transfer of h-BN to Si(111) for materials characterization is similar to previously reported techniques for transfer of CVD grown graphene from Cu[34] and is detailed elsewhere.[6]

The h-BN films were characterized with scanning electron microscopy (SEM) (Leo 1530 FESEM) with an accelerating voltage of 5 kV for morphological analysis prior to transfer (as-grown) as well as after transfer. Following transfer, the films are characterized with optical ellipsometry (Gaertner L116C) for thickness measurements, assuming a bulk refractive index for h-BN of 1.67, while atomic force microscopy (AFM) (Bruker Icon) with a scan rate of 0.5 Hz and a resolution of 512 points per line was used for surface roughness measurements. For structural analysis, select h-BN films were transferred to 3 mm diameter 200 mesh lacey carbon TEM grids or were cross-sectioned (using a focus ion beam (FIB)) for high-resolution transmission electron microscopy (TEM) (JEOL 2010F). Additionally, select h-BN films, both as-grown on copper and transferred to Si(111), were characterized with X-ray photoelectron spectroscopy (XPS) (Kratos Axis Ultra) utilizing an Al Kα X-ray source with energy of 1486 eV for chemical bonding and stoichiometry analysis. For electrical breakdown measurements of h-BN films grown on Cu, the films were transferred to Si/SiO_2(300 nm)/Ti(10 nm)/Au(500 nm) substrates. Contacts (Ti/Au 20/100 nm) with nominal sizes of 500, 250, and 125 μm were deposited over the h-BN film using a shadow mask and an e-beam evaporator (Kurt J. Lesker, Lab-18). Breakdown measurements were then performed with a Keithley 4200 semiconductor characterization system between the 125 μm pads.

■ ASSOCIATED CONTENT

Supporting Information

Photographs of the copper enclosure experimental setup and growth rate data as a function of time and precursor concentration and additional characterization of h-BN films, including XPS, AFM, cross-sectional TEM, and electrical breakdown analysis. This material is available free of charge via the Internet at http://pubs.acs.org/.

■ AUTHOR INFORMATION

Corresponding Author

*E-mail: jrobinson@psu.edu.

Author Contributions

The manuscript was written through contributions of all authors. All authors have given approval to the final version of the manuscript. All authors contributed equally.

Notes

Any opinions, findings, conclusions, or recommendations expressed in this material are those of the authors and do not necessarily reflect the views of the sponsors.

The authors declare no competing financial interest.

■ ACKNOWLEDGMENTS

This work was supported by the Office of Naval Research, Contract N00014-12-C-0124, and the Defense Threat Reduction Agency, Contract HDTRA1-10-1-0093. Support for the WiteC Raman system, Leo 1530 SEM, Bruker Icon AFM, Kratos Axis Ultra XPS, JEOL 2010F TEM, and nanofabrication facility was provided by the National Nanotechnology Infrastructure Network at Penn State. Funding for M.S.B. provided by the Applied Research Laboratory (ARL) Exploratory and Foundational research assistantship.

■ REFERENCES

(1) Dean, C. R.; Young, A. F.; Meric, I.; Lee, C.; Wang, L.; Sorgenfrei, S.; Watanabe, K.; Taniguchi, T.; Kim, P.; Shepard, K. L.; Hone, J. Boron Nitride Substrates for High-Quality Graphene Electronics. *Nat. Nanotechnol.* **2010**, *5*, 722−726.

(2) Kim, E.; Yu, T.; Sang Song, E.; Yu, B. Chemical Vapor Deposition-Assembled Graphene Field-Effect Transistor on Hexagonal Boron Nitride. *Appl. Phys. Lett.* **2011**, *98*, No. 262103.

(3) Gannett, W.; Regan, W.; Watanabe, K.; Taniguchi, T.; Crommie, M. F.; Zettl, A. Boron Nitride Substrates for High Mobility Chemical Vapor Deposited Graphene. *Appl. Phys. Lett.* **2011**, *98*, No. 242105.

(4) Wang, H.; Taychatanapat, T.; Hsu, A.; Watanabe, K.; Taniguchi, T.; Jarillo-Herrero, P.; Palacios, T. BN/Graphene/BN Transistors for RF Applications. *IEEE Electron Device Lett.* **2011**, *32*, 1209−1211.

(5) Lee, K. H.; Shin, H.-J.; Lee, J.; Lee, I.-Y.; Kim, G.-H.; Choi, J.-Y.; Kim, S.-W. Large-Scale Synthesis of High-Quality Hexagonal Boron Nitride Nanosheets for Large-Area Graphene Electronics. *Nano Lett.* **2012**, *12*, 714−718.

(6) Bresnehan, M. S.; Hollander, M. J.; Wetherington, M.; LaBella, M.; Trumbull, K. A.; Cavalero, R.; Snyder, D. W.; Robinson, J. A. Integration of Hexagonal Boron Nitride with Quasi-freestanding Epitaxial Graphene: Toward Wafer-Scale, High-Performance Devices. *ACS Nano* **2012**, *6*, 5234−5241.

(7) Hollander, M. J.; Agrawal, A.; Bresnehan, M. S.; LaBella, M.; Trumbull, K. A.; Cavalero, R.; Snyder, D. W.; Datta, S.; Robinson, J. A. Heterogeneous Integration of Hexagonal Boron Nitride on Bilayer Quasi-Free-Standing Epitaxial Graphene and its Impact on Electrical Transport Properties. *Phys. Status Solidi A* **2013**, *6*, 1062−1070.

(8) Bresnehan, M. S.; Hollander, M. J.; Wetherington, M.; Wang, K.; Miyagi, T.; Pastir, G.; Snyder, D. W.; Gengler, J. J.; Voevodin, A. A.; Mitchel, W. C.; Robinson, J. A. Prospects of Direct Growth Boron Nitride Films as Substrates for Graphene Electronics. *J. Mater. Res.* **2014**, *29*, 459−471.

(9) Nag, A.; Raidongia, K.; Hembram, K. P. S. S.; Datta, R.; Waghmare, U. V.; Rao, C. N. R. Graphene Analogues of BN: Novel Synthesis and Properties. *ACS Nano* **2010**, *4*, 1539−1544.

(10) Preobrajenski, A. B.; Vinogradov, A. S.; Mårtensson, N. Monolayer of h-BN Chemisorbed on Cu(111) and Ni(111): The Role of the Transition Metal 3d States. *Surf. Sci.* **2005**, *582*, 21−30.

(11) Song, L.; Ci, L.; Lu, H.; Sorokin, P. B.; Jin, C.; Ni, J.; Kvashnin, A. G.; Kvashnin, D. G.; Lou, J.; Yakobson, B. I.; Ajayan, P. M. Large Scale Growth and Characterization of Atomic Hexagonal Boron Nitride Layers. *Nano Lett.* **2010**, *10*, 3209−3215.

(12) Guo, N.; Wei, J.; Fan, L.; Jia, Y.; Liang, D.; Zhu, H.; Wang, K.; Wu, D. Controllable Growth of Triangular Hexagonal Boron Nitride Domains on Copper Foils by an Improved Low-Pressure Chemical Vapor Deposition Method. *Nanotechnology.* **2012**, *23*, No. 415605.

(13) Kim, K. K.; Hsu, A.; Jia, X.; Kim, S. M.; Shi, Y.; Dresselhaus, M.; Palacios, T.; Kong, J. Synthesis and Characterization of Hexagonal Boron Nitride Film as a Dielectric Layer for Graphene Devices. *ACS Nano* **2012**, *6*, 8583−8590.

(14) Shi, Y.; Hamsen, C.; Jia, X.; Kim, K. K.; Reina, A.; Hofmann, M.; Hsu, A. L.; Zhang, K.; Henan, L.; Juang, Z.-Y.; Dresselhaus, M. S.; Li, L.-J.; Kong, J. Synthesis of Few-Layer Hexagonal Boron Nitride Thin Film by Chemical Vapor Deposition. *Nano Lett.* **2010**, *10*, 4134−4139.

(15) Yang, P. C.; Prater, J. T.; Liu, W.; Glass, J. T.; Davis, R. F. The Formation of Epitaxial Hexagonal Boron Nitride on Nickel Substrates. *J. Electron. Mater.* **2005**, *34*, 1558−1564.

(16) Kim, K. K.; Hsu, A.; Jia, X.; Kim, S. M.; Shi, Y.; Hofmann, M.; Nezich, D.; Rodriguez-Nieva, J.; Dresselhaus, M.; Palacios, T.; Kong, J. Synthesis of Monolayer Hexagonal Boron Nitride on Cu Foil Using Chemical Vapor Deposition. *Nano Lett.* **2012**, *12*, 161−166.

(17) Britnell, L.; Gorbachev, R. V.; Jalil, R.; Belle, B. D.; Schedin, F.; Katnelson, M. I.; Eaves, L.; Morozov, S. V.; Mayorov, A. S.; Peres, N. M. R.; Castro Neto, A. H.; Leist, J.; Geim, A. K.; Ponomarenko, L. A.; Novoselov, K. S. Electron Tunneling through Ultrathin Boron Nitride Crystalline Barriers. *Nano Lett.* **2012**, *12*, 1707−1710.

(18) Lee, G.-H.; Yu, Y.-J.; Lee, C.; Dean, C.; Shepard, K. L.; Kim, P.; Hone, J. Electron Tunneling Through Atomically Flat and Ultrathin Hexagonal Boron Nitride. *Appl. Phys. Lett.* **2011**, *99*, No. 243114.

(19) Li, X.; Magnuson, C. W.; Venugopal, A.; Tromp, R. M.; Hannon, J. B.; Vogel, E. M.; Colombo, L.; Ruoff, R. S. Large-Area Graphene Single Crystals Grown by Low-Pressure Chemical Vapor Deposition of Methane on Copper. *J. Am. Chem. Soc.* **2011**, *133*, 2816−2819.

(20) Ohring, M. *Materials Science of Thin Films, Deposition & Structure*; Academic Press: San Diego, Ca, 2002.

(21) Yates, B.; Overy, M. J.; Pirgon, O. The Anisotropic Thermal Expansion of Boron Nitride I. Experimental Results and Their Analysis. *Philos. Mag.* **1975**, *32*, 847−857.
(22) Pease, R. S. An X-ray Study of Boron Nitride. *Acta Crystallogr.* **1952**, *5*, 356−361.
(23) Batsanov, S. S. The E-phase of Boron Nitride as a Fullerene. *Combust., Explos. Shock Waves.* **1998**, *34*, 106−108.
(24) Pokropivny, V. V.; Skorokhod, V. V.; Oleinik, G. S.; Kurdyumov, A. V.; Bartnitskaya, T. S.; Pokropivny, A. V.; Sisonyuk, A. G.; Sheichenko, D. M. Boron Nitride Analogs of Fullerenes (the Fulborenes), Nanotubes, and Fullerites (the Fulborenites). *J. Solid State Chem.* **2000**, *154*, 214−222.
(25) Golberg, D.; Bando, Y.; Stéphan, O.; Kurashima, K. Octahedral Boron Nitride Fullerenes Formed by Electron Beam Irradiation. *Appl. Phys. Lett.* **1998**, *73*, 2441−2443.
(26) Daintith, J. *A Dictionary of Chemistry*, 6th ed.; Oxford University Press: Oxford, U.K., 2008.
(27) McLellan, R. B.; Shuttleworth, R. The Vapor Pressure of Solid Copper. *Metallkunde* **1960**, *51*, 149.
(28) Tao, L.; Lee, J.; Chou, H.; Holt, M.; Ruoff, R. S.; Akinwande, D. Synthesis of High Quality Monolayer Graphene at Reduced Temperature on Hydrogen-Enriched Evaporated Copper (111) Films. *ACS Nano* **2012**, *6*, 2319−2325.
(29) Nagashima, A.; Tejima, N.; Gamou, Y.; Kawai, T.; Oshima, C. Electronic Structure of Monolayer Hexagonal Boron Nitride Physisorbed on Metal Surfaces. *Phys. Rev. Lett.* **1995**, *75*, 3918−3921.
(30) Ismach, A.; Chou, H.; Ferrer, D. A.; Wu, Y.; McDonnell, S.; Floresca, H. C.; Covacevich, A.; Pope, C.; Piner, R.; Kim, M. J.; Wallace, R. M.; Colombo, L.; Ruoff, R. S. Toward the Controlled Synthesis of Hexagonal Boron Nitride Films. *ACS Nano* **2012**, *6*, 6378−6385.
(31) Brożek, T.; Szmidt, J.; Jakubowski, A.; Olszyna, A. Electrical Behaviour and Breakdown in Plasma Deposited Cubic BN Layers. *Diamond Relat. Mater.* **1994**, *3*, 720−724.
(32) Sarajlic, O. I.; Mani, R. G. Mesoscale Scanning Electron and Tunneling Microscopy Study of the Surface Morphology of Thermally Annealed Copper Foils for Graphene Growth. *Chem. Mater.* **2013**, *25*, 1643−1648.
(33) Li, X.; Magnuson, C. W.; Venugopal, A.; An, J.; Suk, J. W.; Han, B.; Borysiak, M.; Cai, W.; Velamakanni, A.; Zhu, Y.; Fu, L.; Vogel, E. M.; Voelkl, E.; Colombo, L.; Ruoff, R. S. Graphene Films with Large Domain Size by a Two-Step Chemical Vapor Deposition Process. *Nano Lett.* **2010**, *10*, 4328−4334.
(34) Li, X.; Cai, W.; An, J.; Kim, S.; Nah, J.; Yang, D.; Piner, R.; Velamakanni, A.; Jung, I.; Tutuc, E.; Banerjee, S. K.; Colombo, L.; Ruoff, R. S. Large-Area Synthesis of High-Quality and Uniform Graphene Films on Copper Foils. *Science* **2009**, *324*, 1312−1314.